Eur Radiol (2002) 12:2781–2793
DOI 10.1007/s00330-001-1301-2

MRI of the cartilage

H. Imhof
I.-M. Nöbauer-Huhmann
C. Krestan
A. Gahleitner
I. Sulzbacher
S. Marlovits
S. Trattnig

Received: 14 May 2001
Revised: 29 November 2001
Accepted: 4 December 2001
Published online: 19 March 2002

H. Imhof (✉) · I.-M. Nöbauer-Huhmann
C. Krestan · A. Gahleitner · S. Marlovits
S. Trattnig
Department of Osteology,
Universitätklinik für Radiodiagnostik,
AKH-Vienna, Waehringer Guertel 18–20,
1090 Vienna, Austria
e-mail: mr@univie.ac.at
Tel.: +43-1-404005803
Fax: +43-1-40003777

I. Sulzbacher
Universitätsklinik für Pathologie Vienna,
Waehringer Guertel 18–20, 1090 Vienna,
Austria

Abstract With the introduction of fat-suppressed gradient-echo and fast spin-echo (FSE) sequences in clinical routine MR visualization of the hyaline articular cartilage is routinely possible in the larger joints. While 3D gradient-echo with fat suppression allows exact depiction of the thickness and surface of cartilage, FSE outlines the normal and abnormal internal structures of the hyaline cartilage; therefore, both sequences seem to be necessary in a standard MRI protocol for cartilage visualization. In diagnostically ambiguous cases, in which important therapeutic decisions are required, direct MR arthrography is the established imaging standard as an add-on procedure. Despite the social impact and prevalence, until recent years there was a paucity of knowledge about the pathogenesis of cartilage damage. With the introduction of high-resolution MRI with powerful surface coils and fat-suppression techniques, visualization of the articular cartilage is now routinely possible in many joints. After a short summary of the anatomy and physiology of the hyaline cartilage, the different MR imaging methods are discussed and recommended standards are suggested.

Keywords Cartilage · Anatomy · MRI

Introduction

With the introduction of high-resolution MRI with powerful surface coils and fat-suppression techniques, visualization of the articular cartilage is now routinely possible in many points. Cartilage damage is very well visualized. This prominent position of MRI in diagnosis and staging of cartilage lesions is due to the newest developments in cartilage repair. Advances in molecular biology have put MRI in an even more prominent clinical position.

Anatomy and physiology of the hyaline cartilage

The term "hyaline" cartilage refers, somewhat misleadingly, to the amorphous, homogeneous appearance of cartilage matrix by light microscopy; however, cartilage is actually quite fibrous and demonstrates marked 3D anisotropy. Cartilage can be divided into four (or five) zones, depending on the differentiation of the most superficial zone into one or two compartments, and is based on the morphology and arrangement of chondrocytes and the staining properties of the matrix. The deepest layer, representing 5% of the entire volume, is calcified and serves to anchor an extensive network of collagen fibrils that radiate toward the surface in dense bundles linked together by bridging fibrils. More superficially, the collagen fibrils become thinner and more randomly organized, with numerous, obliquely oriented fibrils to resist the shearing forces that arise there. Ultimately, the fibrils band together at the articular surface to form a compact, tangentially arranged layer that is relatively impermeable to water. This fine network of collagen fibrils is further organized into parallel leaves or laminae that radiate vertically from the calcified zone. Superficially, these laminae become thinner and arch over to form highly packed horizontal leaves at the articular surface (Fig. 1) [1, 2, 3, 4, 5, 6].

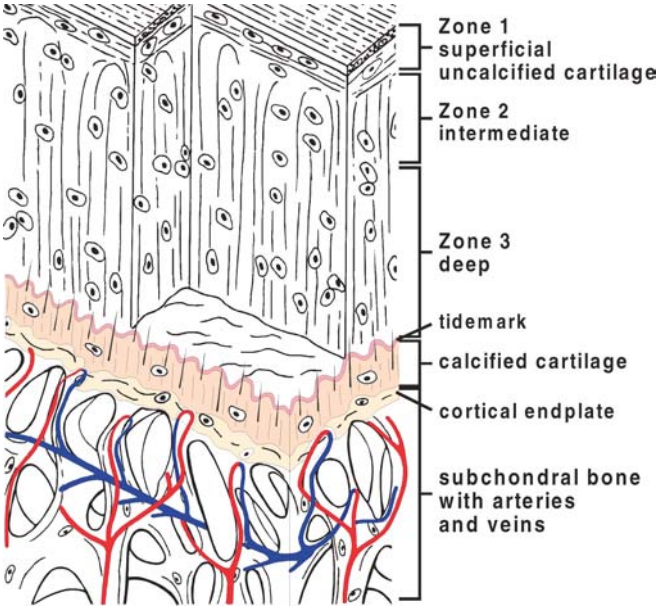

Fig. 1 Different layers of hyaline cartilage and subchondral bone with vessels. Figures 1, 2, and 3 are from [63]

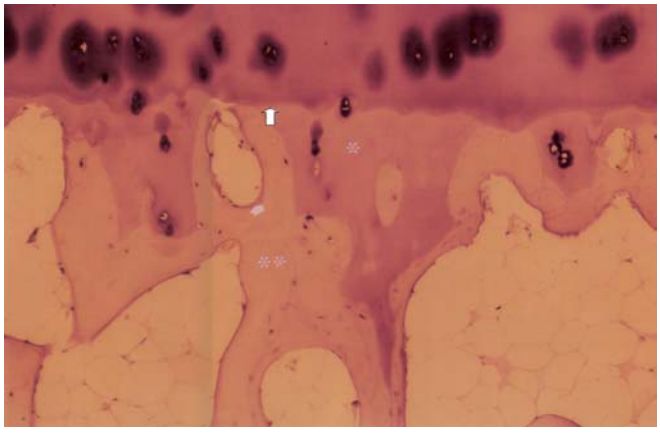

Fig. 2 Histological section with hematoxylin and eosin staining. The tidemark (*solid arrow*) borders calcified and uncalcified cartilage and represents the mineralization front. The calcified cartilage is connected to the cortical endplate. A subchondral vessel reaches the tidemark (*open arrow*)

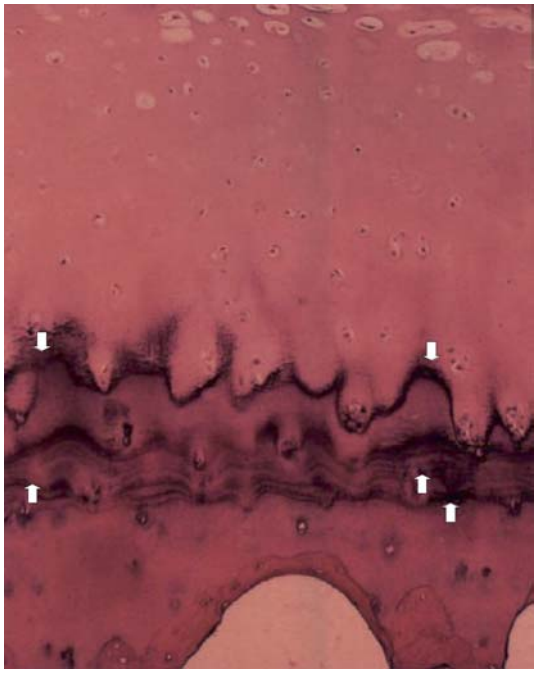

Fig. 3 Histological section of hyaline cartilage with duplication of the tide mark (*arrows*)

Between the deep calcified zone and the uncalcified cartilage lies the so-called tide mark representing the mineralized front of the calcified cartilage (Fig. 2). In case of severe stress with overloading, the mineralization zone can be duplicated or even multifolded. This is due to a quick repair process that builds new mineralization fronts leaving behind deep zones of uncalcified cartilage (Fig. 3). The chondrocytes produce the collagen fibrils and as ground substance proteoglycans. The distribution of proteoglycans within the cartilage matrix is related to mechanical requirements. This distribution varies markedly from joint to joint, geographically within a single articular cartilage, and as a function of age. There are structural changes in proteoglycans that occur during aging that differ from those of degenerative osteoarthritis.

The negatively charged proteoglycans of the cartilage exert osmotic pressure to draw water into the cartilage, which counteracts mechanical pressures, forces water out, and produces an expansion pressure that is resisted by the tension in the collagen fibers. Under physiological conditions, the stiff collagen fibers prevent proteoglycans from taking up water maximally [2, 3, 4].

The extreme smooth surface of the hyaline cartilage serves as gliding surface with a very low resistance. The elasticity of the hyaline cartilage is, only to a very small degree, a load cushion. The majority of the load forces are usually taken up by the subchondral bone (30%), whereas normal hyaline cartilage takes only 1–3% of the load forces. In addition to its "lubricant" task, hyaline cartilage dissipates loading forces to a larger surface, which lowers the maximal load. It must also be emphasized that the subchondral bone and hyaline cartilage are a functional unit in load dissipation and uptake, vascularization, nutrition, and repair mechanisms. During physiologic articular loading and unloading, the cartilage and subchondral region are deformed. This maintains nutrition. Complete immobilization with steady unloading results in decreased synthesis of proteoglycans and fibrils by the chondrocytes and loss of cartilage. Conversely,

exercise increases synthesis, leading to thickening and swelling of cartilage.

Normal replacement of cartilage begins from the calcified cartilage, which, throughout life, has the same thickness. Calcified cartilage is absorbed from the subchondral side by invading tiny vessels, as it advances into the uncalcified cartilages. This leads to constant remodelling of the joint and reduces the incongruency of the joints. Increasing joint congruency with aging diminishes physiologic loading, unloading, and nutrition, and may be one cause of aging. Uncalcified cartilage may become thinner with age.

Imaging

The purpose of cartilage imaging is to visualize the surface of the cartilage, as well as its matrix thickness, volume, and subchondral borders. Currently, MRI is the standard imaging method for this purpose.

T1-weighted spin-echo (SE) imaging can depict boundaries between cartilage and subchondral bone but is relatively poor at demonstrating cartilage–fluid interfaces (Fig. 4) [7]. In a non-blinded study of naturally occurring lesions in 20 cadaveric knees, only 70% of lesions were detectable [8]. With conventional T2-weighted spin-echo-sequences the signal of cartilage decreases much faster than that of joint fluid. This mismatch increases the contrast between cartilage and effusion; however, the signal-to-noise ratio is generally insufficient to support high spatial resolution. Furthermore, the preferential loss of signal from the deep layers of cartilage with long echo times obscures the interface between cartilage and subchondral bone, which makes it difficult to obtain an accurate measurement of cartilage thickness or volume [9, 10]. One study demonstrated only a 52% accuracy rate with conventional T2-weighted SE sequences to detect naturally occurring lesions in the patello-femoral joints of cadaver [10].

In high-field MRI (7.05 T), short-TE projection reconstruction MR microscopy proved to be reliable for measurements of cartilage thickness in an ex vivo study [11]. The signal in cartilage is highly dependent on the relative orientation of its collagen fibers, and moreover the deep layer of the cartilage shows rapid signal decay due to short T2 relaxation times. The good result has been attributed to the ability to use short TE to obtain MR signal also from structures with short T2. As the deep layer of cartilage was homogeneously hyperintense, the delineation from the hypointense tidemark/cortical bone was improved.

Fast spin-echo (FSE) imaging combines the heavy T2-weighting, magnetization transfer effects and relative preservation of high signal intensity in the marrow fat to produce images in which articular cartilage has extremely low signal intensity, whereas joint fluid and subchondral bone exhibit high signal intensity. Thus, contrast between cartilage and adjacent joint fluid and bone marrow is high [12]; however, the boundary between the calcified deepest layer of cartilage, which can thicken in cases of degeneration, and the subchondral bone may be obscured. Since FSE sequences allow multiple acquisitions to be obtained within a reasonable imaging time, T2-weighted FSE imaging can provide sufficient signal-to-noise ratio to allow a high in-plane resolution matrix (Fig. 5). The unusual T2 behavior of cartilage is exclusively due to the presence and organization of collagen [13, 14]. Collagen, with a highly regular structure, tends to immobilize water molecules and promote dipolar interactions between their protons, thus accelerating T2 relaxation.

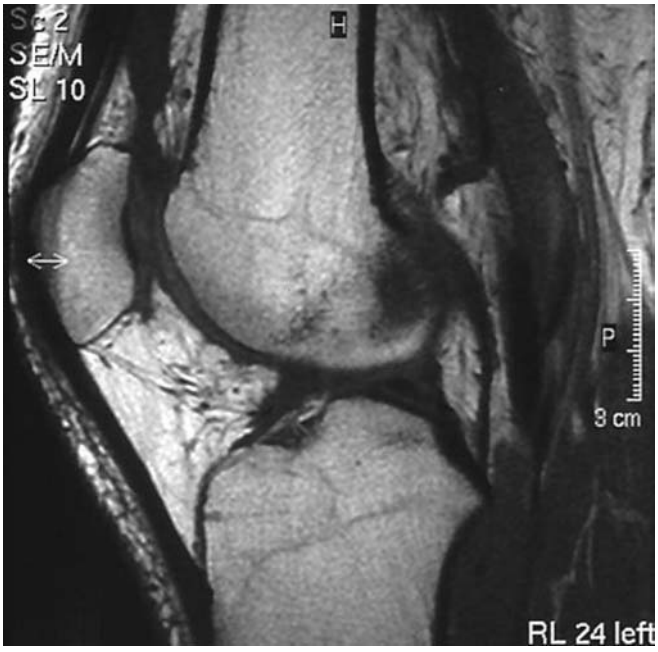

Fig. 4 Magnetic resonance imaging of the knee joint (T1-weighted spin echo): Boundaries between uncalcified cartilage and subchondral bone (including calcified cartilage) are well demonstrated. Boundaries between cartilage and synovial fluid are not recognizable

An ex vivo study using magnetic resonance microscopy (MRM) showed a good correlation between a trilaminar appearance of the cartilage and histology [15]. In this study, a hypointense superficial layer, an intermediate hyperintense layer, and a deep hypointense layer were found. The authors claimed that the different signal intensities might represent the different concentration of collagen concentration, which are maximum in the superficial and in the deep layer. A 90° rotation around the longitudinal axis of the bone led to loss of trilaminar appearance, which was attributed to the different (anisotropic) collagen fiber orientation, thus leading to a reduced dipole-to-dipole interaction with a corresponding in-

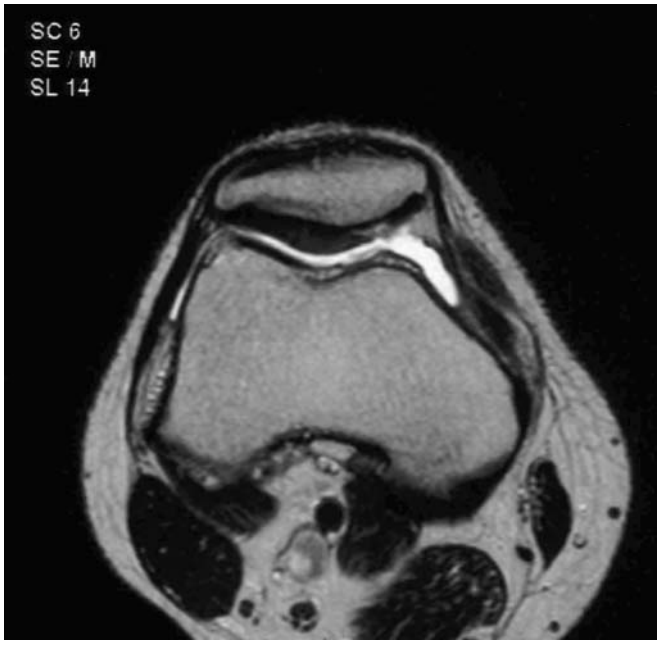

Fig. 5 Magnetic resonance imaging of the knee joint (axial T2-weighted fast spin echo, FSE): hyaline cartilage with a hyperintense focal defect on the medial patellar cartilage of the femoral joint shows an extremely low signal, which contrasts strongly to the high signal intensity of joint fluid as well as to the relatively bright fatty marrow signal

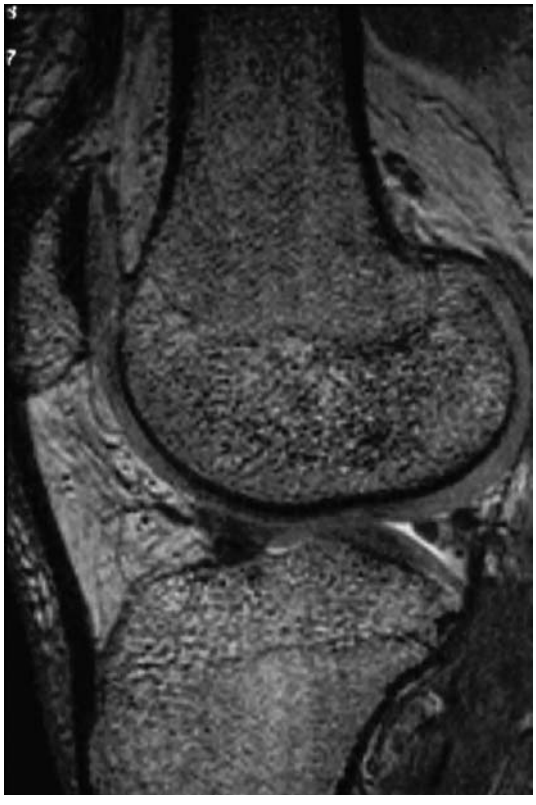

Fig. 6 Magnetic resonance imaging of the knee joint (reversed pulse sequence of fast imaging steady precession DESS, lateral): The hyaline cartilage exhibits an intermediate signal, whereas joint fluid has a high signal intensity. Solid tissues, such as menisci, are not well delineated

crease in T2 relaxation. T2-weighted FSE sequences are therefore useful not only due to the high contrast between cartilage and adjacent synovial fluid for the detection of surface defects, but also for the detection of early matrix damage, potentially at a stage at which cartilage is still salvageable [16].

Because of the multiple refocusing 180° radiofrequency pulses, the T2-weighted FSE sequence is relatively insensitive to magnetic susceptibility artifacts, which may be important in patients who have undergone previous arthroscopy and ligamentous reconstruction, and can be used to accurately detect associated meniscal and ligamentous pathology.

However, FSE imaging as a two-dimensional sequence is limited to a minimum section thickness of 3 mm. Thinner slices (2 mm) can now be obtained with two-dimensional FSE sequences on higher performance gradient subsystems, which are currently becoming commercially available; however, multiplanar reconstructions, which are often important in evaluating the curved structures in joints, cannot be performed.

Gradient-echo (GRE) sequences with a longer TE decrease the relative signal intensity of cartilage and improve cartilage fluid contrast but only at the cost of signal-to-noise ratio and, therefore, spatial resolution. Moreover, due to magnetic susceptibility artifacts from the deep calcified layer of cartilage and cancellous subchondral bone, long TE GRE sequences obscure the cartilage bone interface and make quantification of cartilage difficult [17, 18]. Clinical studies using such sequences have reported poor results with sensitivities ranging from a low of 31% to a high of 87% [19].

Gradient-echo sequences with short TE suffer from poor contrast between cartilage and joint fluid; thus, additional contrast must be available. A possibility offered by one manufacturer is the combination of a standard fast imaging steady precession (FISP) sequence with PSIF, the reversed pulse sequence of FISP, which results in the double-echo steady-state (DESS) sequence. With this sequence, in addition to the GRE sequence, T2*-weighting is achieved by transverse magnetization from steady-state components and from the high-frequency (PSIF) pulse. The PSIF part of the sequence leads to high T2 contrast, whereas the FISP part provides representative morphological images. As a result, joint fluid exhibits high signal intensity and provides a better delineation of cartilage surface, as the cartilage has a medium signal intensity (Fig. 6). Since a 3D technique is possible with this sequence, thin contiguous slices can be obtained; however, there are some disadvantages with this

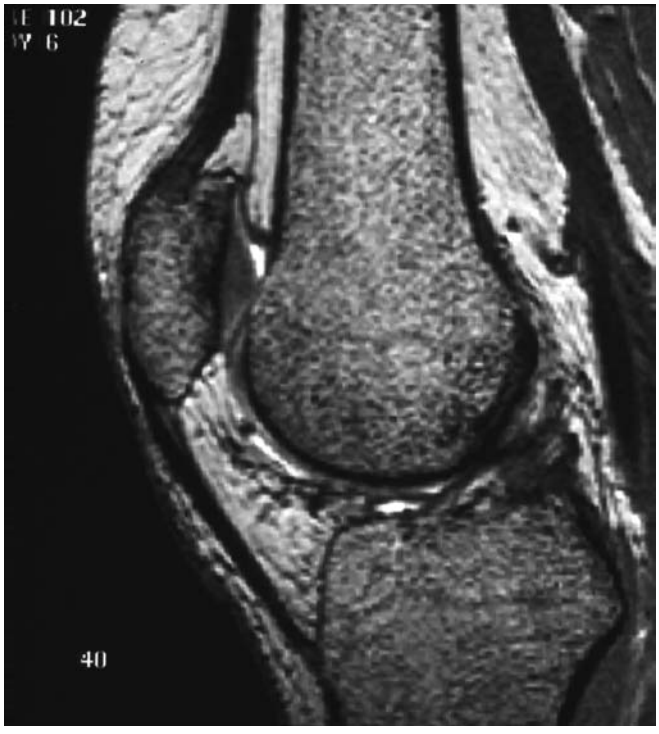

Fig. 7 Magnetic resonance imaging of the knee joint (double-echo steady-state, DESS): There is a poor contrast between articular cartilage and solid surrounding tissue

technique. Firstly, a significant amount of joint fluid is necessary for optimal delineation of cartilage surfaces, which is not always present. Secondly, the contrast-to-noise ratio between cartilage and solid surrounding tissue, in particular menisci, is low, which poses a problem in delineation and segmentation for volume measurements. By combining DESS with selective water excitation in principle an indirect fat suppression is performed; however, since synovial fluid is also strongly enhanced by this technique, the contrast-to-noise ratio between the hyperintense articular cartilage and bright synovial fluid is poor (Fig. 7) [20]. In this study the 3D DESS sequence thus was found to be only moderately accurate in detecting patellar cartilage abnormalities. It proved to be superior to sagittal TSE for the detection of cartilage softening, but not for the detection of surface lesions. For cartilage softening, the sensitivity of 3D DESS was better than that of TSE (73 vs 53%). The same was true for the specificity (75 vs 65%), and the accuracy (70 vs 62%). For surface lesions, the values for TSE were 43 vs 60%, 92 vs 92%, and 83 vs 86%, respectively. In another study [21], A_z values [area under the receiver operating characteristics (ROC) curves] for water-excited 3D DESS and 3D fast low-angle shot (FLASH) were 0.96, which was significantly higher than for all 2D pulse sequences.

The addition of frequency-selective fat suppression to 3D spoiled GRE sequences results in a significant increase in contrast-to-noise ratio between cartilage and joint fluid and cartilage and subchondral bone, demonstrating articular cartilage as a band of high signal intensity. After suppression of fat, signal intensities are rescaled by the MR unit to render articular cartilage the brightest structure in the joint, with joint fluid and subchondral bone demonstrating a relatively lower signal intensity (Fig. 8).

In a recent study, a trilaminar appearance was attributed to a truncation artifact on a fat-suppressed 3D spoiled GRE sequence [22]. This phenomenon is most apparent in the phase-encoding direction at interfaces at which there is an abrupt and marked change in signal intensity. When there are two such interfaces a summation effect occurs which is observed as a thin hypointense line within the central tissue.

The advantage of fat-suppressed 3D spoiled GRE sequences is the relatively high signal intensity of articular cartilage in contrast to low signal intensity from the surrounding tissue (Fig. 9). Three-dimensional acquisition

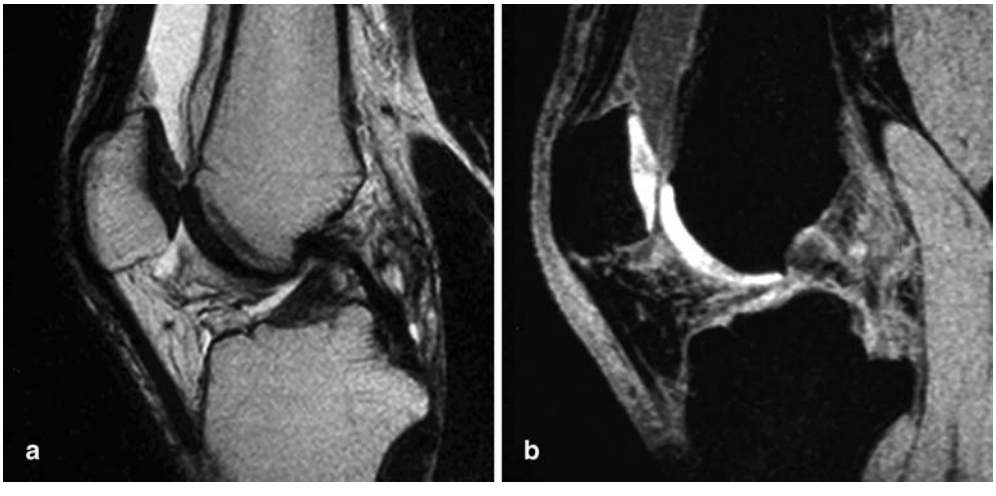

Fig. 8 Same patient as in Fig. 7 **a** (T2-weighted FSE): The central patellar cartilage lesion is slightly hyperintense. **b** (3D GRE with fat suppression): Hyaline cartilage is a band of high signal intensity with a focal hypointense lesion within the patellar cartilage. Synovial fluid and subchondral bone (with calcified cartilage) show a lower signal intensity

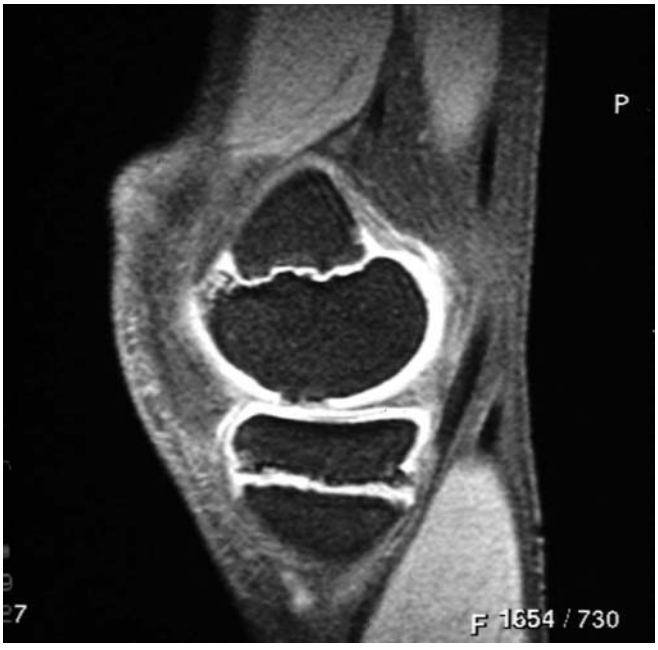

Fig. 9 Magnetic resonance imaging of the knee joint in a 4-year-old boy, after trauma (3D GRE with fat suppression): Hyaline cartilage is bright including the growth plate. There is a posttraumatic defect in the femoral cartilage. (From [64])

yields images with higher resolution and contrast-to-noise ratio than two-dimensional acquisitions. Thin imaging sections allow high-quality multiplanar reconstructions which are useful to evaluate the patellar and trochlear surfaces with images perpendicular to facets where the articular surface is curved. Finally, thin-section volume acquisitions allow segmentation and accurate 3D reconstructions of articular cartilage (Fig. 10) [10, 23, 24, 25, 26].

Fat-suppressed, 3D spoiled GRE imaging is easy to perform, widely available, and, contrary to other cartilage imaging techniques, such as magnetization transfer imaging, it requires no postprocessing of data and avoids misregistration artifacts.

The use of a fat-suppressed, 3D spoiled GRE sequence has been shown to result in an accuracy of 91%, a sensitivity of 87%, and a specificity of 97% [24]. As with other techniques, the highest accuracy was achieved with the patello-femoral joint and higher-grade defects were detected with greater accuracy. A major drawback is the relatively long examination time of 10–15 min, which makes it less attractive for routine clinical use. To decrease the scan time, faster and stronger gradients are now available. Moreover, examination time can be reduced by using selective water excitation instead of spectral presaturation. To speed up examination time, a recently developed 3D multishot echo planar imaging (EPI) sequence with fat suppression can be used for evaluation of the hyaline articular cartilage. The performance of the fat-suppressed 3D EPI sequence and the 3D GRE sequence with fat suppression in the evaluation of articular cartilage was compared using histology as a reference. Both sequences showed comparable performance, but the scan time for the EPI sequence was reduced by a factor of four which makes it more suitable for clinical routine [27].

In a clinical study [28], fat-suppressed 3D FLASH sequence, however, was less precise for grading of cartilage lesions than CT arthrography, which was used as a reference. Moreover, it did not show as many fissures.

The 3D spoiled GRE sequence with fat suppression provides 3D information that is useful for determining the volume and 3D configuration of cartilage [29, 30, 31]. Thin-section acquisition allows accurate volumetric measurements not only of the cartilage layers of the knee joint, but also of smaller joints with an accuracy of 5% and an interobserver variability of 3.3–9.6%. Newer results show a variation of only 1.9% [32]. These measurements may be helpful in the serial evaluation of disorders that affect cartilage integrity diffusely and in conditions that cause progressive cartilage loss such as osteoarthritis and inflammatory arthropathies [33].

Subtraction magnetization transfer (MT) contrast imaging can also show the hyaline cartilage with positive contrast [34]. Magnetization transfer contrast is a relatively new technique that alters MR image contrast by means of a relaxation mechanism different from that of conventional T1-, T2-, or T2*-weighted imaging (Fig. 11). In this technique, continuous or pulsed radiofre-

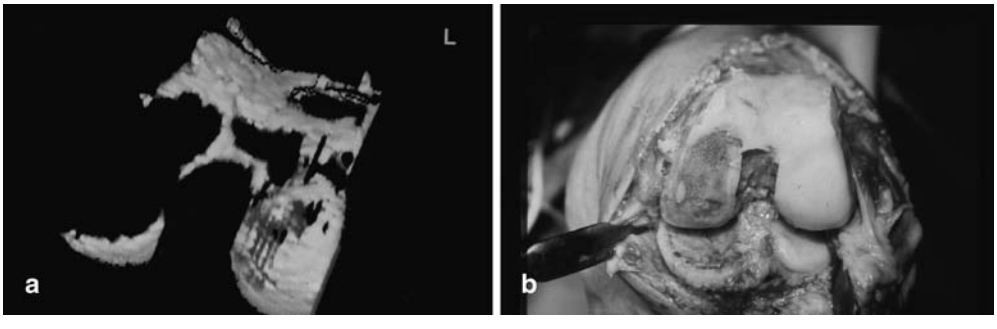

Fig. 10 **a** A 3D reconstruction of the hyaline cartilage of the knee joint with multiple defects based on 3D GRE with fat suppression. **b** Macromorphological image of the multiple defects seen in **a**

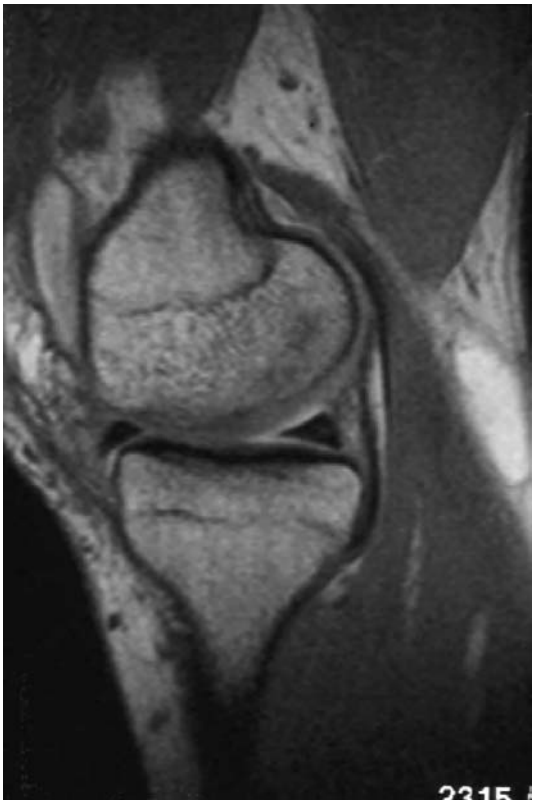

Fig. 11 T2*-weighted GRE with magnetization transfer prepulses. The significant decrease in signal intensity of the hyaline cartilage allows better delineation

quency irradiation is applied during a standard MR imaging sequence to selectively saturate protons with restricted mobility associated with an increase in macromolecules. The T2 decay in the macromolecular pool is too rapid to contribute signal to conventional MR images. This MR-invisible pool is, however, in thermodynamic equilibrium with the MR visible pool of mobile protons in bulk water within the same tissue. Cross-relaxation magnetization transfer can occur between the two pools. Selective saturation of the macromolecular protons perturbs this equilibrium and evokes a net transfer of magnetization from the water protons to the macromolecular pool. Since the macromolecular protons do not contribute to the signal in the MR image, this magnetization transfer manifests as a loss of signal intensity in tissues in which these two proton pools are tightly coupled. Woolf et al. [35] demonstrated that a significant amount of MT occurs in articular cartilage, whereas no significant MT occurs in synovial fluid. With T2*-weighted GRE sequences, these changes can be used to produce increased contrast between high signal intensity cartilage compared with standard sequences [33]. Subtraction of MR imaging data obtained with a pulsed MT technique from that obtained without an MT technique generates images in which contrast reflects tissue differences in MT. This technique depicts the hyaline articular cartilage as a band of high signal intensity tissue contrasted to adjacent low signal intensity joint fluid and subchondral bone, similar to the fat-suppressed 3D GRE sequences [34]; however, this technique is not widely available, requires post-processing of the data, and can result in misregistration artifacts due to changes in patient positioning. The latter artifact could be significantly reduced by the development of a so-called dynamic MTC, which means that within one sequence non-MTC and MTC scans can be acquired, and misregistration artifacts are eliminated.

Table 1 Direct MR arthrography. The amount of contrast agent required depends on the joint to be examined

Joint	Volume of contrast agent (ml)[a]
Shoulder	10–25
Elbow	5–15
Wrist	2–7
Hip	10–20
Knee	20–40
Ankle	4–12
Talomalleolar joint	2–4

[a] 2-mmol dilute solutions of gadolinium

Magnetization transfer is a collagen-dependent mechanism to achieve signal loss in cartilage. Disruption or loss of the collagen matrix in cartilage results not only in a small increase in proton density, but also eliminates the attenuating effects of collagen-dependent T2 relaxation and MT. As a result, the signal intensity increases in areas of matrix damage or early chondromalacia, which theoretically, offers a technique for visualization of early cartilage disease. Unfortunately, MT with current instrumentation results only in a moderate contrast-to-noise ratio; thus, this technique has not proven to be superior to other available MR imaging techniques [36].

The transfer of magnetization from protons in tissue water to protons in collagen also can unintentionally be caused by off-resonance irradiation of neighboring slices during conventional multislice imaging. This effect increases with the number of slices used and is most pronounced in FSE imaging because of the multiple 180° refocusing pulses used in this technique [37].

The detection rate for cartilage lesions without surface defects by MTC MR imaging was 80%, corresponding to an increased collagen concentration [38].

The use of gadolinium compounds for the imaging of articular cartilage has been applied in several different forms. Direct MR arthrography, where a 2-mmol dilute solution containing gadolinium compounds is injected directly into the joint (with or without the help of X-ray fluoroscopy), dramatically improves contrast between cartilage and arthrographic fluid [39]. The amount of contrast medium used depends on the investigated joint and can vary from 1 to 3 ml, to 15 to 25 ml (Table 1).

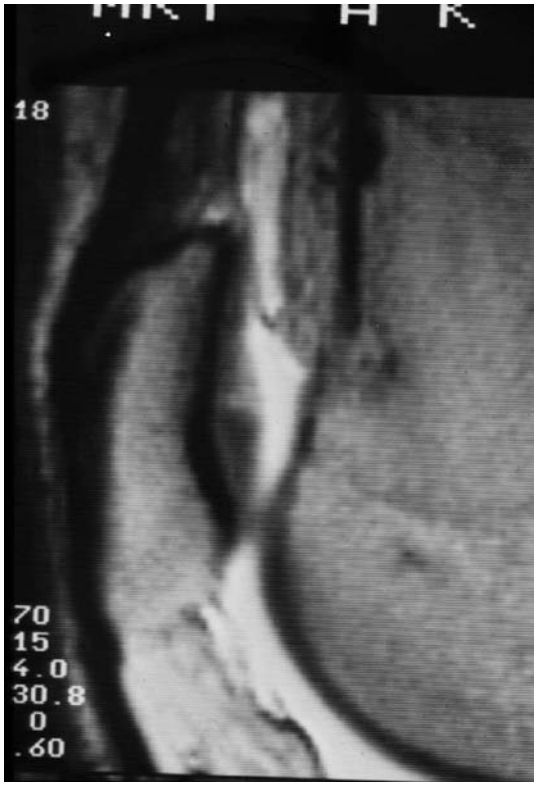

Fig. 12 Knee joint (direct MR arthrography, T1-weighted SE): The synovial fluid is hyperintense. There is a cartilage defect within the patella representative of first-stage chondromalacia

After injection of the contrast medium, the joint should be moved to ensure an even distribution of the contrast medium (Fig. 12). The examination should be finished 30–45 min after the intra-articular injection to avoid increased dilution of contrast medium. Moreover, the contrast medium might be taken up by cartilage, thus lowering the delineation of the surface of the cartilage [39]. Magnetic resonance arthrography (MRA) has proved to be 100% specific for FISP and T1-weighted sequences, and very sensitive, with detection rates of 87 and 85% [40]. The accuracy of the method was 88 and 87% for both sequences, respectively.

Direct MRA is routinely used as an adjunct in diagnostically ambiguous MRI examinations, where a definitive diagnosis is mandatory (e.g., before surgery).

The only other imaging modality that offers potential as an equally diagnostic alternative to standard MRA is the newly "re-developed multi-slice" CT arthrography.

Indirect MRA, with a less invasive intravenous injection of 5–15 ml 0.1 mmol gadolinium compounds, has also been used; however, with this method, there are many inherent disadvantages, including less contrast, enhancement of overlying structures, and no capsular expansion. These disadvantages prevent the widespread use of this method; thus, indirect MR arthrography may be limited to those cases in which an invasive procedure is contraindicated or where the absence of a fluoroscopy unit renders direct arthrography impractical.

Quantitative 3D analysis of cartilage

Quantitative image processing and analysis techniques play an increasingly important role in evaluating cartilage loss and monitoring response to medical and surgical therapy [41, 42, 43]. Several investigators have reported the use of 3D reconstructions of the articular cartilage with subsequent volumetric quantification of the entire cartilage surface. With this technique, cartilage is segmented from the surrounding tissues using a signal-intensity-based thresholding technique applied to a cartilage-sensitive MRI sequence [44]. In the knee joint, the intraobserver reproducibility error for measurements of 3D cartilage volumes have been reported to range between 3.6 and 6.4%, and the interobserver error was 7.8% in the same study. For the tibial cartilage morphometry, spoiled 3D GRE sequence with selective water excitation, the precision of volume and mean thickness measurements was between 2.3 and 2.6% in healthy volunteers and patients with severe osteoarthritis, whereas the precision was lower for maximal tibial cartilage thickness [45]. Recent developments proved that specific MR sequences (3D FT spoiled gradient-recalled acquisition in the steady state) allow very sensitive reproduction of quantitative cartilage measurements [43].

Postoperative imaging of cartilage repair

With recent advances in the treatment of articular cartilage disorders, including osteochondral autografts and autologous chondrocyte implantation, noninvasive MRI has gained additional importance with the determination of the structural success of surgical intervention.

In the assessment of different cartilage repair techniques, proton-density and T2-weighted FSE sequences have proved to be most useful in the postoperative follow-up. Cartilage transplants should be evaluated with respect to their morphology and signal intensity. For morphology the degree of defect repair (filling of the defect), the integration to the border zone (possible demarcation border to the surrounding cartilage), the surface of the transplant, the subchondral lamina, and the subchondral bone should be evaluated.

The signal intensity of the osteochondral autograft ("mosaicplasty") shows marked hyperintensity on T2-weighted FSE images in the early postoperative period (3–6 months), representing edema. Conversion to similar signal intensity in comparison with the native hyaline cartilage over a period of approximately 6–12 months is caused by development of fibrovascular tissue. Within

the follow-up period of 18 months, however, many transplanted osteochondral autografts still showed a fissure-like gap to the neighboring original cartilage, indicating that the transplant had still not been integrated. Other problems were the lack of development of new cartilage at the donor site (demonstrated by MRI), and the difficulty to find sufficient donor sites in patients potentially in need of cartilage transplants. Consequently, young patients with acute (traumatic) cartilage lesions should have been exclusively selected for transplantation of osteochondral autografts.

For chondrocyte transplantation, 3D cell transplants are cultivated ex vivo, subsequently implanted after local application of growth factors. The signal intensity of the chondrocyte autograft shows conversion of marked hyperintensity on T2-weighted FSE images in the early postoperative period to similar signal intensity in comparison with the native hyaline cartilage, probably representing transformation into hyaline cartilage, over a period of approximately 6–12 months (S. Marlovits and S. Trattnig, pers. commun.). Magnetic resonance imaging shows smoothening of the border between transplanted and original cartilage, indicating integration. One possible future problem could be a constant cartilage overgrowth. The problem to differentiate between a normal from a abnormal signal behavior of the transplant in the postoperative course is not yet solved, but recent studies show that the use of more sophisticated techniques, such as delayed contrast-enhanced techniques or diffusion-weighted imaging, may be more helpful in the definition of an intact transplant.

Future developments

The glycosaminoglycans (GAG) of the hyaline cartilage comprise approximately 5% of tissue weight. The GAGs are a constitutive part of proteoglycans. The basis of dGEMRIC is the following: GAGs have abundant charge side groups that confer a negative fixed charge density (FCD) to the cartilage matrix. Mobile ions distribute in the tissue to reflect the local GAG concentration. In particular, dGEMRIC is concerned with the distribution of the negatively charged MRI contrast agent Gd(DTPA)2. If injected intravenously, the contrast agent will penetrate cartilage from both the synovial surface as well as from bone [46, 47], and will then distribute into areas of cartilage that are depleted of GAG at a higher concentration than in areas of high GAG [48]. GD(DTPA)2 has a concentration-dependent effect on the MR parameter T1; therefore, T1 images in the presence of Gd(DTPA)2 reflect the Gd(DTPA)2 concentration, and hence tissue GAG concentration. (It is important to emphasize that this use of Gd(DTPA)2 – to measure GAG in the tissue requires penetration of Gd(DTPA)2 – into the tissue, and thus this method, differs from those which use the contrast agent to better delineate anatomic defects early after injection.).

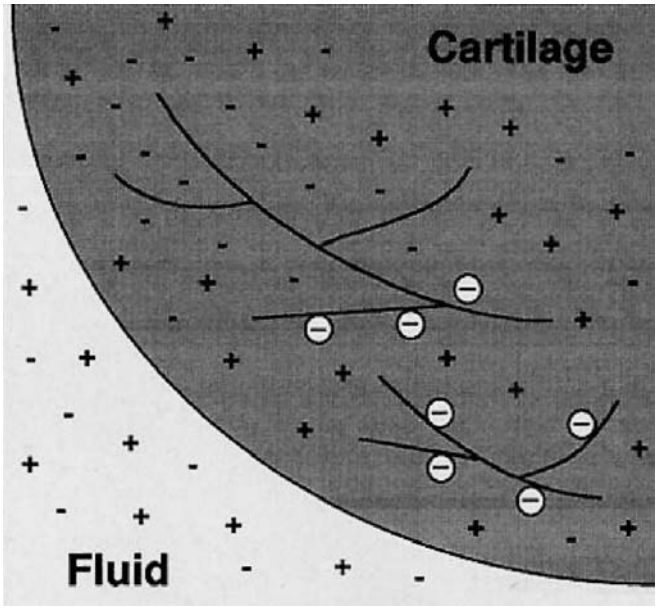

Fig. 13 Graphic presentation of the normal ion distribution. Negatively charged GAG moieties (*white*), and otherwise evenly distributed ions within the cartilage and synovial fluid

dGEMRIC has been validated both in vitro and in vivo as a non-destructive surrogate of histologic analysis of GAG distribution in cartilage [46, 48, 49, 50, 51]. A clinical protocol for dGEMRIC has been recommended [47], and pilot clinical studies have been applied to the evaluation of osteoarthritis in knees [47, 52, 53] as well as dysplasia in hips [54]. The GAGs represent one of the major macromolecular constituents of cartilage and are critical to this mechanical support function, and thus are presumed to be necessary for a fully functional ACT implant.

These GAGs have moieties that are ionized under physiological conditions. In degenerative osteoarthritis the amount of GAGs decreases with the intensity of the disease.

Ionic contrast medium applied intravenously as double-dose Gd-DTPA^{-2} is distributed in relation to the GAG concentration. The even or uneven distribution within the cartilage takes between 45 and 270 min depending on the investigated joint and location. In normal (healthy) cartilage, the uptake will be very low, and in cartilaginous disorders, uptake due to the lack of charged GAGs is high.

In the future, this method could allow visualization of abnormal cartilage tissue at a very early stage in rheumatoid and degenerative diseases (Figs. 13, 14).

The GAGs could also directly or indirectly affect contrast in other imaging methods. The GAGs contribute to the MT effect in cartilage [55, 56]; however, this effect is

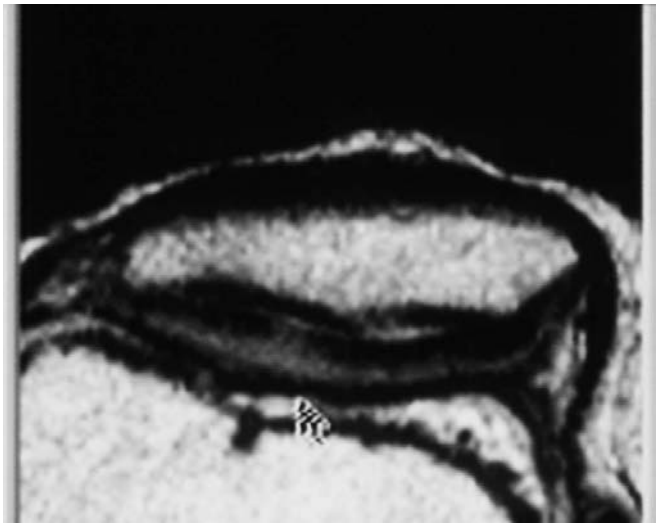

Fig. 14 Magnetic resonance imaging of the patellar cartilage (3 T; T1-weighted SE), 120 min after i.v. ionic contrast application: diffusion of contrast medium into the cartilage (*arrow*)

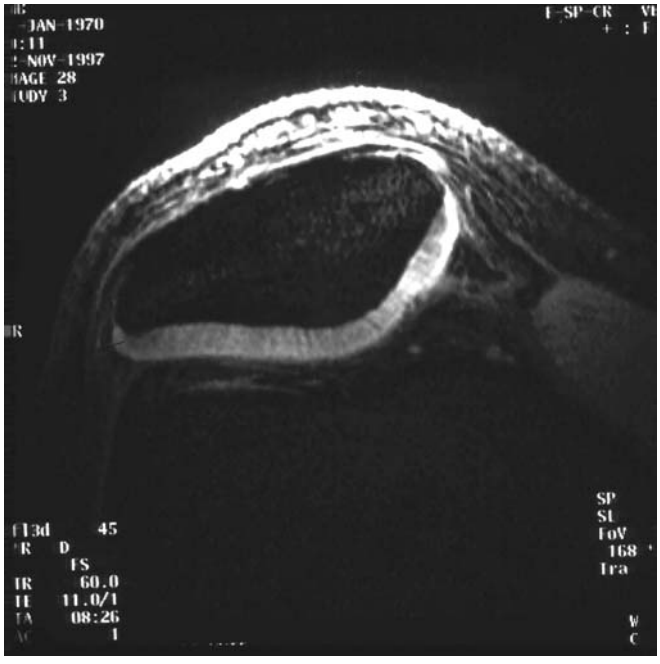

Fig. 15 Magnetic resonance imaging of the patellar cartilage (high-resolution 3D GRE with fat suppression): radial matrix of the patellar cartilage

very small relative to the effect of collagen on MT, and therefore it may be difficult to use MT to follow changes in cartilage disease.

Cartilage is essentially a fluid-filled "sponge" comprising approximately 75% of cartilage weight. In early disease, the percentage of water in cartilage goes up by a few percent. The cause of hydration changes remain unclear but includes the loss of or damage to solid matrix elements. Changes in hydration can be seen directly by obtaining a proton-density-weighted image. Unfortunately, the sensitivity is very low, given the relatively small changes in hydration with diseases.

T1 and T2 relaxation times depend on hydration [57, 58]. T2 may be very sensitive to hydration changes and is used to identify focal cartilage lesions.

Interpretation of T2 differences, however, requires caution. Differences in T2 across the cartilage may, in part, reflect collagen orientation issues due to the "magic angle" effect [59]; therefore, suggested cartilage T2-mapping still requires further clinical evaluation. In addition, the interpretation of T2 differences is complicated because of the non-mono-exponential behavior of T2 in cartilage. Altogether the false-positive rate could be quite high.

The diffusion coefficient of water in cartilage also increases with increased hydration. Since hydration generally increases with cartilage degeneration, the diffusion coefficient of water would be expected to track degeneration [60, 61]. Unfortunately, high-precision diffusion measurements are technically difficult due to motion artifacts and cannot be used routinely as yet.

Use of high-resolution surface coils may improve the detail resolution of the cartilage matrix. Initial results have demonstrated that the radial structure of hyaline cartilage can be depicted (Figs. 14, 15).

Optical coherence tomography (OCT) might be another promising method to achieve high-resolution images in cartilage disease [62]. Similar to ultrasound, it measures the intensity of backreflected infrared light. The axial resolution is very high (5–15 μm). As the method had originally been developed for imaging the transparent tissues of the eye, the imaging penetration in non-transparent tissues is limited to approximately 4 mm. Cartilage has, to date, only been imaged in osteoarthritis in vitro. As OCT is optical fiber based, it could be integrated with arthroscopes. A possible future application might therefore be the use as an additional tool in arthroscopy.

Recommended MR imaging standards

Although there are still innumerable new cartilage sequences (e.g., fluctuating equilibrium magnetic resonance, FEMR) reported each year, the generally accepted MR imaging standard is dual FSE and 3D GRE with fat suppression. While FSE allows visualization of intracartilaginous structural abnormalities, 3D GRE outlines the thickness and surface of uncalcified cartilage, synovial fluid, and subchondral bone, together with calcified cartilage. The 3D reconstruction is easily performed in all dimensions with 3D GRE. In unclear cases where an exact (pretherapeutic) diagnosis is warranted, direct MR arthrography is the unsurpassed method of choice (Tables 2, 3).

Table 2 Technical principles. *FSE* fast spin echo; *GRE* gradient echo; *PD* proton density; *FOV* field of view

Direct MR arthrography. Sequences that have been established for visualization of cartilage lesions	
Imaging protocol	Indication
T2 FSE (PD T2-weighted)	Intrachondral lesion
3D GRE+FSE	Surface defects
Technical details	
Small FOV, large matrix size	
Slice thickness ≤2 mm (with 3D:1.5–1/mm)	
Two or more planes	
Surface coil	

Pathologies that require cartilage imaging

The following pathologies require cartilage imaging:

1. Degenerative osteoarthritis before invasive therapies
2. Follow-up of cartilage/subchondral region
3. Osteochondritis dissecans/osteonecrosis
4. Rheumatoid disease before invasive therapies
5. Cartilage/subchondral fractures (including metaphyseal fractures)
6. Cartilaginous blastomas
7. Rare metabolic diseases (e.g., calcium pyrophosphate dihydrate, gout)

Table 3 Advantages and disadvantages of the sequences recommended in Table 2

	Advantages	Disadvantages
3D GRE+FSE	High contrast/noise ratio	Long examination time
	Cartilage/joint effusion	Insensitive to bone marrow edema and subchondral cysts
	Cartilage/bone marrow	Sensitive to susceptibility artifacts
	High resolution (out of plane)	
	Multiplanar reconstructions	
	Volumetric measurements	
Dual FSE	High contrast/noise ratio	Hyperintense bone marrow
	Cartilage/joint effusion	Limited out-of-plane resolution
	Cartilage/bone marrow	No multiplanar reconstructions
	High resolution (in-plane)	
	Less sensitive to susceptibility artifacts	
	Excellent subchondral imaging	

References

1. Bullough PG (1992) Atlas of orthopaedic pathology. Gower, London
2. Maroudas A (1979) Physiochemical properties of articular cartilage. In: Freeman MAR (ed) Adult articular cartilage. Pitman Medical, England
3. Maroudas A, Bayliss MT, Venn MF (1980) Further studies on the composition of human femoral head cartilage. Ann Rheum Dis 39:514–523
4. Cochran G (1988) Orthopädische Biomechanik. Enke, Stuttgart
5. Ekholm R, Ingelmark BE (1952) Functional thickness variations of human articular cartilage. Acta Soc Med Ups 57:39–59
6. Brown TD, Radin EL, Martin RB, Burr DB (1984) Finite element studies of some juxtaarticular stress changes due to localized subchondral stiffening. J Biomech 17:11–24
7. Hayes CW, Conway WF (1992) Evaluation of articular cartilage: radiographic and cross-sectional imaging techniques. Radiographics 12:409–442
8. Hodler J, Berthiaume MJ, Schweitzer ME, Resnick D (1992) Knee joint hyaline cartilage defects: a comparative study of MR and anatomic sections. J Comput Assist Tomogr 16:597–603
9. McCauley MR, Kier R, Lynch KJ, Jokl P (1992) Chondromalacia patellae: diagnosis with MR imaging. Am J Roentgenol 158:101–105
10. Recht MP, Kramer J, Marcelis S, Pathria MN, Trudell D, Haghighi P, Sartoris DJ, Resnick D (1993) Abnormalities of articular cartilage in the knee: analysis of available MR techniques. Radiology 187:473–478
11. Cova M, Toffanin R, Szomolanyi P, Vittur F, Pozzi-Mucelli RS, Jellus V, Silveestri F, Dalla-Palma L (2000) Short-TE projection reconstruction MR-microscopy in the evaluation of articular cartilage thickness. Eur Radiol 10:1222–1226
12. Constable RT, Anderson AW, Zhong J, Gore JC (1992) Factors influencing contrast in fast spin-echo MR imaging. Magn Reson Imaging 10:497–511
13. Xia Y (2000) Magic-angle effect in magnetic resonance imaging of articular cartilage: a review. Invest Radiol 35:602–621
14. Mlynarik V, Trattnig S (2000) Physiochemical properties of normal articular cartilage and its MR appearance. Invest Radiol 35:589–594
15. Cova M, Toffanin R, Frezza F, Pozzi-Mucelli M, Mlynarik V, Pozzi-Mucelli RS, Vittur F, Dalla-Palma L (1998) Magnetic resonance imaging of articular cartilage: ex vivo study on normal cartilage correlated with magnetic resonance microscopy. Eur Radiol 8:1130–1136
16. Potter HG, Linlater JM, Allen AA, Hannafin JA, Haas SB (1998) MR imaging of articular cartilage in the knee: a prospective evaluation utilizing fast spin-echo imaging. J Bone Joint Surg [Am] 80:1276–1284
17. Heron CW, Calvert PT (1992) Three-dimensional gradient-echo MR imaging of the knee: comparison with arthroscopy in 100 patients. Radiology 183:839–844

18. Speer KP, Spritzer CE, Goldner JL, Garrett WE (1991) Magnetic resonance imaging of traumatic knee articular cartilage injuries. M J Sports Med 19:396–402
19. Wojtys E, Wilson M, Buckwalter K, Braunstein E, Martel W (1987) Magnetic resonance imaging of knee hyaline cartilage and intraarticular pathology. Am J Sports Med 15:455–463
20. Ruehm S, Zanetti M, Romero J, Hodler J (1998) MRI of patellar articular cartilage: evaluation of an optimized gradient echo sequence (3D-DESS) J Magn Reson Imaging 8:1246–1251
21. Wörtler K, Strothmann M, Tombach B, Reimer P (2000) Detection of articular cartilage lesions: experimental evaluation of low- and high-field-strength MR imaging at 0.18 and 1.0 T. J Magn Reson Imaging 11:678–685
22. Erikson SJ, Waldschmidt JG, Czervionke LF, Prost RW (1996) Hyaline cartilage: truncation artifacts as a cause of trilaminar appearance with fat-suppressed three-dimensional spoiled gradient recalled sequences. Radiology 201:260–264
23. Recht MP, Piraino DW, Paletta GA, Schils JB, Belhobek GH (1996) Accuracy of fat-suppressed three-dimensional spoiled gradient-echo FLASH MR imaging in the detection of patellofemoral articular cartilage abnormalities. Radiology 198:209–212
24. Disler DG, McCauley TR, Wirth CR, Fuchs MD (1995) Detection of knee hyaline cartilage defects using fat-suppressed three-dimensional spoiled gradient-echo MR imaging: comparison with standard MR imaging and correlation with arthroscopy. Am J Roentgenol 165:377–382
25. Sittek H, Eckstein F, Gavazzeni A, Milz S, Kiefer B, Schulte E, Reiser M (1996) Assessment of normal patella cartilage volume and thickness using MRI: an analysis of currently available techniques. Skeletal Radiol 25:55–62
26. Chandnani VP, Ho C, Chu P, Trudell D, Resnick D (1991) Knee hyaline cartilage evaluated with MR imaging: a cadaveric study involving multiple imaging sequences and intraarticular injection of gadolinium and saline solution. Radiology 178:557–561
27. Trattnig S, Huber M, Breitenseher MJ, Trnka H-J, Rand T, Kaider A, Helbich T, Imhof H, Resnick D (1998) Imaging articular cartilage defects with 3D fast-suppressed echo-planar imaging: comparison with conventional 3D fat-suppressed gradient echo sequence and correlation with histology. J Comput Assist Tomogr 22:8–14
28. Daenen BR, Ferrara MA, Marcelis S, Dondelinger RF (1998) Evaluation of patellar cartilage surface lesions: comparison of CT arthrography and fat-suppressed FLASH 3D MR imaging. Eur Radiol 8:981–985
29. Marshall KW, Mikulits DJ, Guthrie BM (1995) Quantitation of articular cartilage using magnetic resonance imaging and three-dimensional reconstruction. J Bone Joint Surg 13:814–823
30. Pilch L, Stewart C, Gordon D, Inman R, Parsons K, Pataki I, Stevens J (1994) Assessment of cartilage volume in the femorotibial joint with magnetic resonance imaging and 3D computer reconstruction. J Rheumatol 21:2307–2320
31. Eckstein F, Sittek H, Gavazzeni A, Schulte E, Milz S, Kiefer B, Reiser M, Putz R (1996) Magnetic resonance chondrocrassometry (MR CCM): a method for accurate determination of articular cartilage thickness. Magn Reson Med 35:89–96
32. Watt I (2000) Arthrosis: a single or many diseases? Radiologe 40:1134–1140 [in German]
33. Peterfy CG, van Dijke CF, Lu Y, Nguyen A, Connick TJ, Kneeland JB, Tirman PF, Lang P, Dent S, Genant HK (1995) Quantification of the volume of articular cartilage in the metacarpophalangeal joints of the hand: accuracy and precision of three-dimensional MR imaging. Am J Roentgenol 165:371–375
34. Peterfy CG, Majumdar S, Lang P, van-Dijke CF, Sack K, Genant HK (1994) MR imaging of the arthritic knee: improved discrimination of cartilage, synovium and effusion with pulsed saturation transfer and fat-suppressed T1-weighted sequences. Radiology 191:413–419
35. Woolf SD, Chesnick S, Frank JA, Lim KO, Balaban RS (1991) Magnetization transfer contrasts: MR imaging of the knee. Radiology 170:623–628
36. Potter HG, Schweitzer ME, Attchek DW (1997) Advances in orthopedic imaging: pitfalls and new application. Instr Course Lect 46:521–539
37. Yao L, Gentili A, Thomas A (1996) Incidental magnetization transfer contrast in fast spin-echo imaging of cartilage. J Magn Reson Imaging 1:180–184
38. Vahlensieck M, Dombrowski F, Leutner C, Wagner U, Reiser M (1994) Skeletal Radiol 23:535–539
39. Engel A (1990) Magnetic resonance knee arthrography. Acta Orthop Scand (Suppl 240) 61: 1–57
40. Kramer J, Recht MP, Imhof H, Engel A (1994) MR contrast arthrography (MRA) in assessment of cartilage lesions. J Comput Asssist Tomogr 18:218–224
41. Eckstein F, Westhoff J, Sittek H, Maag KP, Haubner M, Faber S, Englmeier KH, Reiser M (1998) In vivo reproducibility of three-dimensional cartilage volume and thickness measurements with MR imaging. Am J Roentgenol 170:593–597
42. Losch A, Eckstein F, Haubner M, Englmeier KH (1997) A non-invasive technique for 3-dimensional assessment of articular cartilage thickness based in MRI. I. Development of a computational method. Magn Reson Imaging 15:795–804
43. Lang P, Yoshioka H, Steines D, Nöbauer-Huhmann I-M, Imhof H (2000) Magnetresonanztomographie (MRT) des Gelenkknorpels: aktueller Wissensstand und neue Entwicklungen. Radiologe 40:1141–1148
44. Peterfy CG, van Dijke CF, Janzen DL, Gluer CC, Namba R, Majumdar S, Lang P, Genant HK (1994) Quantification of articular cartilage in the knee with pulsed saturation transfer subtraction and fat-suppressed MR imaging: optimization and validation. Radiology 192:485–491
45. Hylik-Durr A, Faber S, Burgkart R, Stammberger T, Maag KP, Englmeier KH, Reiser M, Eckstein F (2000) Precision of tibial cartilage morphometry with a coronal water-excitation MR sequence. Eur Radiol 10:297–303
46. Bashir A, Gray M, Boutin R, Burstein D (1997) Glycosaminoglycanin articular cartilage: in vivo assessment with delayed Gd(DTPA)2-enhanced MR imaging. Radiology 205:551–558
47. Burstein D, Velyvis J, Scott K, Kim Y, Jaramillo, Boutin R, Gray M (2001) Protocol issues for delayed Gd(DTPA)2-enhanced MRI (dGEMRIC) for clinical evaluation of articular cartilage. Magn Reson Med 45:36–41
48. Bashir A, Gray M, Burstein D (1996) Gd-DTPA2 – as a measure of cartilage degradation. Magn Reson Med 36:665–673
49. Bashir A, Gray M, Hartke J, Burstein D (1995) Nondestructive imaging of human cartilage glycosaminoglycan concentration by MRI. Magn Res Med 41:857–865
50. Mlynarik V, Trattnig S, Humber M, Zembsch A, Imhof H (1999) The role of relaxation times in monitoring proteoglycan depletion in articular cartilage. J Magn Reson Imaging 10:497–502
51. Trattnig S, Mlynarik V, Breitenseher M, Huber M, Zembsch A, Rand T, Imhof H (1999) MRI visualization of proteoglycan depletion in articular cartilage via intravenous of Gd-DTPA. Magn Reson Imaging 17:577–583

52. Tiderius CJOL, Leander P, DeVerdier H, Dahlberg L (1999) Gadolinium (Gd-DTPA) enhanced MRI can differentiate between arthroscopically healthy and degenerated human knee cartilage. In: Orthopaedic Res Society, p 439
53. Dahlberg LNF, Olsson LE, Verdier H, Leander P (2000) Contrast-enhanced MRI in cartilage repair. International Cartilage Repair Society, Gothenburg, p 147
54. Kim YJ, Jarmillo D, Burstein D, Gray ML, Millis MB (2000) Delayed gadolinium enhanced magnetic resonance imaging of hip joint articular cartilage: correlation with clinical symptoms. Radiological Society of North America, Chicago, p 451
55. Gray ML, Burstein D, Lesparance LM, Gehrke L (1995) Magnetization transfer in cartilage and its constituent macromolecules. Magn Reson Med 34:319–325
56. Wachsmuth L, Juretschke HP, Raiss RX (1997) Can magnetization transfer magnetic resonance imaging follow proteoglycan depletion in articular cartilage? Magma 5:71–80
57. Lui AK (1995) The dependence of NMR measured diffusion, magnetization transfer, and T2 relaxation on fractional water content in bovine articular cartilage (Thesis). In: Electrical engineering and computer science. Massachusetts Institute of Technology Cambridge
58. Dardzinski BJ, Mosher TJ, Li S, Van Slyke MA, Smith MB (1997) Spatial variation of T2 in human articular cartilage. Radiology 205:546–550
59. Wacker FK, Bolze X, Felsenberg D, Wolf KJ (1998) Orientation-dependent changes in MR signal intensity of articular cartilage: a manifestation of the "magic angle" effect. Skeletal Radiol 27:306–310
60. Burstein D, Gray ML, Hartman AL, Gipe R, Foy BD (1993) Diffusion of small solutes in cartilage as measured by nuclear magnetic resonance (NMR) spectroscopy and imaging. J Orthop Res 11:465–478
61. Xia Y, Farquhar T, Burton-Wurster N, Vernier-Singer M, Lust G, Jelinski LW (1995) Self-diffusion monitors degraded cartilage. Arch Biochem Biophys 323:323–328
62. Herrmann JM, Pitris C, Bouma BE, Boppart SA, Jesser CA, Stamper DL, Fujimoto JG, Brezinski ME (1999) High resolution imaging of normal and osteoarthritic cartilage with optical coherence tomography. J Rheumatol 26:627–635
63. Imhof H, Sulzbacher I, Grampp S, Czerny C, Youssefzadeh S, Kainberger F (2000) Subchondral bone and cartilage disease. Invest Radiol 35:581–588
64. Trattnig S, Mlynarik V, Huber M, Ba-Ssalamah A, Puig S, Imhof H (2000) Magnetic resonance imaging of articular cartilage and evaluation of cartilage disease. Invest Radiol 35:595–601